Reconstruction of frozen-core all-electron orbitals from pseudo-orbitals

Balázs Hetényi,[a] Filippo De Angelis, Paolo Giannozzi,[b] and Roberto Car
Department of Chemistry, Princeton University and Princeton Materials Institute, Princeton, New Jersey 08544

(Received 2 February 2001; accepted 10 July 2001)

We investigate the numerical feasibility of reconstructing frozen-core all-electron molecular orbitals from corresponding pseudo-orbitals. We perform density-functional calculations on simple atomic and molecular model systems using ultrasoft pseudopotentials to represent the atomic cores. We apply a transformation due to Blöchl [Phys. Rev. B **50**, 17953 (1994)] to each calculated pseudo-orbital to obtain a corresponding frozen-core all-electron molecular orbital. Our model systems include the reconstruction of the $5d$ orbital of a gold atom, and the occupied valence states of the TiO_2 molecule. Comparison of the resulting all-electron orbitals to corresponding ones that were obtained from calculations in which the core electrons were explicitly included indicates that all-electron molecular orbital reconstruction is a feasible and useful operation in reproducing the correct behavior of molecular orbitals in the nuclear core regions. © *2001 American Institute of Physics.* [DOI: 10.1063/1.1398097]

I. INTRODUCTION

Electronic structure calculations have contributed greatly to our understanding of molecular and solid-state properties. Many such calculations are based on density-functional theory (DFT).[1,2] A widely used technique in actual electronic structure calculations (including DFT) of extended systems is the pseudopotential (PP) technique,[3,4] which is based on the frozen core (FC) approximation. In FC, the core electrons of a given atom are assumed to be unperturbed by the presence of other atoms in the system. The validity of FC has been investigated analytically[5] and numerically,[6,7] and has been shown to hold in most chemically relevant cases.

PPs are constructed based on FC, so that each atomic nucleus together with its core electrons is represented by an effective potential. In general, the use of PPs offers the advantage that the atomic core electrons do not need to be included in the calculation for the extended system. In the case of plane-wave-based calculations, another advantage is due to the fact that PPs are constructed to have nodeless orbitals for isolated atoms. The orbitals of the extended system that result from the solution of the PP Hamiltonian [i.e., the pseudo (PS) orbitals] are thus less oscillatory in the nuclear core regions than the corresponding solutions of the frozen-core all-electron (FCAE) Hamiltonian; therefore, a smaller set of plane waves can be used in calculating the properties of the extended system.

Since the savings in basis set size is achieved by eliminating the nodes in the nuclear core region, molecular orbitals are significantly altered by the use of PPs in the core regions. In many applications, such as in the calculation of x-ray absorption spectra,[8,9] chemical shifts,[7,10] or hyperfine splittings,[11,12] knowledge of the electronic orbitals or electronic density in atomic core regions is required. Spin polarization of the core contributes to hyperfine splittings. While this effect is usually small compared to the valence contribution, there are cases such as the CH_3 radical where the core contribution is important. In the context of the reconstruction procedure presented here, this contribution can be estimated from an (spherical) atomic calculation once the reconstructed valence spin-polarized orbitals have been obtained. The orbitals obtained from PP Hamiltonians are not adequate to describe these phenomena.

In this paper we investigate the feasibility of reconstructing a FCAE orbital from a PS orbital obtained from a PP calculation. We use a transformation due to Blöchl,[13] which forms the basis of the projector-augmented wave (PAW)[13] method. The PAW method is an FCAE method which is essentially equivalent to the ultrasoft pseudopotential (USPP) formalism of Vanderbilt.[14] While this study focuses on reconstructing FCAE orbitals from ultrasoft PS orbitals, we point out that the procedure used here is applicable in the case of the standard norm-conserving pseudopotential[15] (NCPP) as well, as was done in Ref. 10.

We note that the PAW transformation has been used in reconstructing the density in nuclear core regions in order to calculate hyperfine parameters.[11,12] Furthermore, an extension of the PAW transformation has been used in the calculation of NMR chemical shifts[10] from PP calculations.

We test the FCAE orbital reconstruction procedure by performing a set of plane-wave PP-based DFT calculations on simple model systems and applying the Blöchl transformation to the resulting PS orbitals. For each model system, we also perform independent AE calculations without PPs. For our model systems we choose atomic neon, gold, and the TiO_2 molecule. Since one of the advantages of USPPs is that *d* orbitals are made easier to handle, it is instructive to demonstrate the reconstruction procedure on atomic gold and the TiO_2 molecule.

In the case of atoms, we compare the reconstructed orbitals to orbitals calculated by radial integration of the

[a]Electronic mail: bhetenyi@princeton.edu
[b]On leave from Scuola Normale Superiore, Pisa, Italy.

Kohn–Sham equations. In the case of the TiO_2 molecule, we compare the reconstructed orbitals to orbitals obtained from an all-electron calculation using Gaussian-type orbitals (AE-GTO).[16]

In the following section we describe the Blöchl transformation and aspects of the USPP formalism that are relevant to the reconstruction of the FCAE orbital. In Sec. III we describe the details of our calculations. In Sec. IV we present comparisons of calculated and reconstructed FCAE orbitals for test cases. In Sec. V we draw conclusions. In a later paper we will apply the method presented here to calculate x-ray absorption spectra of condensed matter systems.[9]

II. METHOD

A. Relation between the all-electron orbital and the pseudo-orbital

In this subsection we discuss the Blöchl transformation.[13] The Blöchl transformation is an exact transformation between an FCAE orbital and a corresponding PS orbital in terms of atomic AE and PS partial waves. For the full derivation see Ref. 13.

In the following we denote the FCAE(PS) orbitals of the extended system by $|\Psi_n\rangle(|\tilde{\Psi}_n\rangle)$. The transformation that relates the FCAE and the PS orbitals is given by

$$|\Psi_n\rangle = |\tilde{\Psi}_n\rangle + \sum_i (|\phi_i\rangle - |\tilde{\phi}_i\rangle)\langle \tilde{p}_i|\tilde{\Psi}_n\rangle_{R_i}, \tag{1}$$

where $|\phi_i\rangle$ denotes atomic AE partial waves obtained by integrating the radial Schrödinger equation; $|\tilde{\phi}_i\rangle$ denotes atomic PS partial waves chosen to reproduce the corresponding AE partial waves outside the core radius R_i. The index i in Eq. (1) is a composite index denoting the atomic site $\tilde{\mathbf{R}}_i$, atomic energy level, and angular momentum $\{\varepsilon_i l_i m_i\}$. The notation $\langle|\rangle_{R_i}$ stands for taking the scalar product within the core radius R_i. The atomic PS partial waves are constructed to be nodeless and usually smoother than the atomic AE functions within the core radius. Furthermore, the atomic PS partial waves match continuously onto the atomic AE functions at the core radius.

The functions $|\tilde{p}_i\rangle$ are projector functions to be determined. A condition on the projector functions $\tilde{p}_i$ is arrived at by requiring that an atomic PS orbital transform into an atomic AE orbital. This requirement is satisfied if

$$\langle \tilde{p}_i|\tilde{\phi}_j\rangle_{R_j} = \delta_{ij}. \tag{2}$$

B. The projector function in Vanderbilt's ultrasoft pseudopotential formalism

In this subsection we describe aspects of Vanderbilt's USPP that are relevant in reconstructing AE orbitals. We point out that the projector functions required in Eq. (1) are inherent in the formalism. For the full derivation of the USPP see Refs. 14, 17.

The first step is to carry out an AE calculation on an atom in some reference configuration, usually the ground state. The screened local potential $V_{\mathrm{AE}}(r)$ is stored, and a set of reference states $\{\phi_i\}$ is chosen, where i is a composite index that stands for energy level and angular momentum $\{\epsilon_i l_i m_i\}$. The states are chosen such that their energy levels ϵ_i span the energy range over which good scattering properties are desired (usually the range of occupied bulk valence states). Cutoff radii are chosen for each orbital (R_i) and for the local potential (R_c). Some diagnostic radius R_d that is larger than the cutoff radii is chosen.

An algorithm is used to generate a local potential $V_{\mathrm{loc}}(r)$ which agrees with $V_{\mathrm{AE}}(r)$ outside R_c. As in Eq. (1), an atomic PS partial wave $\tilde{\phi}_i(r)$ is constructed for each $\phi_i(r)$ subject to the constraint that the two functions join smoothly at R_i. Note that norm conservation is not a requirement. Next, a new set of functions

$$|\tilde{\chi}_i\rangle = (\epsilon_i - T - V_{\mathrm{loc}})|\tilde{\phi}_i\rangle, \tag{3}$$

is calculated, where T denotes the one-electron kinetic energy operator. Writing ϵ_i as

$$\epsilon_i = \frac{[T + V_{\mathrm{AE}}(r)]\phi_i(r)}{\phi_i(r)}, \tag{4}$$

and using the facts that

$$\begin{aligned} &V_{\mathrm{loc}}(r) = V_{\mathrm{AE}}(r) \quad \text{if} \quad r > r_c, \\ &\phi_i(r) = \tilde{\phi}_i(r) \quad \text{if} \quad r > r_c, \end{aligned} \tag{5}$$

it is trivial to see that the functions $|\tilde{\chi}_i\rangle$ are localized within the core region. The matrix $B_{ij} = \langle \tilde{\phi}_i|\tilde{\chi}_j\rangle$ is well defined, and can be used to define a set of local functions

$$|\tilde{\beta}_i\rangle = \sum_j (B^{-1})_{ij}|\tilde{\chi}_j\rangle, \tag{6}$$

which satisfies

$$\langle \tilde{\beta}_i|\tilde{\phi}_j\rangle_{R_j} = \delta_{ij}, \tag{7}$$

which is the condition in Eq. (2). The functions $|\tilde{\beta}_i\rangle$ are therefore the projector functions required for the Blöchl transformation [Eq. (1)].

In the case of standard NCPP,[15] the projector functions can be constructed by setting the off-diagonal elements of B_{ij} to zero, and using Eq. (6). The orthogonality condition in Eq. (2) is thus satisfied, since there is one state for each angular momentum component. Note that the projector functions can be used to construct the fully nonlocal PP, as is done in the Kleinman–Bylander transformation.[18] The reconstruction procedure in Ref. 10 was done using such projector functions. We note in passing that there is a general NCPP formalism due to Blöchl,[19] where the construction of projection operators is analogous to that in the USPP formalism.

In order to arrive at the actual form of the USPP, we need to define the quantities

$$Q_{ij}(r) = \phi_i^*(r)\phi_j(r) - \tilde{\phi}_i^*(r)\tilde{\phi}_j(r), \tag{8}$$

and

$$D_{ij} = B_{ij} + \epsilon_j Q_{ij}, \tag{9}$$

where $Q_{ij} = \langle \phi_i|\phi_j\rangle - \langle \tilde{\phi}_i|\tilde{\phi}_j\rangle$.

The full nonlocal pseudopotential has the form

$$V_{US}=\sum_{ij} D_{ij}^{(0)}|\beta_i\rangle\langle\beta_j|, \tag{10}$$

where $D_{ij}^{(0)}$ is obtained by "unscreening" D_{ij} according to

$$D_{ij}^{(0)}=D_{ij}-\int d\mathbf{r}\, V_{\mathrm{loc}}(\mathbf{r})n(\mathbf{r}). \tag{11}$$

The "unscreened" ionic potential is obtained by

$$V_{\mathrm{loc}}^{\mathrm{ion}}(\mathbf{r})=V_{\mathrm{loc}}(\mathbf{r})-\int d\mathbf{r}'\frac{n(\mathbf{r}')}{|\mathbf{r}-\mathbf{r}'|}-\mu_{xc}(\mathbf{r}), \tag{12}$$

where $n(\mathbf{r})$ and $\mu_{xc}(\mathbf{r})$ denote the valence density and the exchange-correlation potential, respectively, and

$$n(\mathbf{r})=\sum_n \langle\tilde{\psi}_n|\mathbf{r}\rangle\langle\mathbf{r}|\tilde{\psi}_n\rangle+\sum_{n(j,k)} Q_{jk}(\mathbf{r})\langle\tilde{\psi}_n|\tilde{\beta}_j\rangle\langle\tilde{\beta}_k|\tilde{\psi}_n\rangle. \tag{13}$$

In the following we calculate AE orbitals by applying the Blöchl transformation in the context of the USPP formalism on PS orbitals obtained from a DFT calculation. We calculate PS orbitals for several model systems in which the atomic cores are represented by USPPs [Eq. (10)], then apply the expression

$$|\Psi_n\rangle=|\tilde{\Psi}_n\rangle+\sum_i (|\phi_i\rangle-|\tilde{\phi}_i\rangle)\langle\tilde{\beta}_i|\tilde{\Psi}_n\rangle, \tag{14}$$

to obtain the corresponding AE orbital.

III. DETAILS OF THE CALCULATIONS

In the following, we test the numerical feasibility of reconstructing FCAE orbitals via the Blöchl transformation. We calculate the FCAE orbitals by first calculating the PS orbitals and then applying the Blöchl transformation [Eq. (1)] to obtain the corresponding FCAE orbitals. In Sec. IV we present comparisons for three test cases: (1) an isolated neon atom ($2s$ and $2p$ orbitals); (2) an isolated gold atom ($5d$ orbital); and (3) TiO_2 molecule (valence orbitals). We also perform an auxiliary calculation on an isolated Ti atom.

To generate the PS orbitals for the three cases, we perform plane-wave DFT[17] calculations using USPPs to represent atomic cores. In all cases we use a simple cubic cell and periodic boundary conditions. Throughout we used the gradient-corrected PW91[20] exchange-correlation functional. The USPP, the atomic AE and PS partial waves, and the projector functions ($\{|\tilde{\beta}_i\rangle\}$) are generated by integrating the radial Kohn–Sham equation on a logarithmic grid.[14,17] This procedure generates the atomic AE orbitals (or partial waves) for all the atoms involved in the three test cases. The resulting atomic AE orbitals are used for comparison in the case of the isolated neon and gold atoms. The energy cutoffs for the plane-wave basis sets in the plane-wave DFT calculation and the sizes of the simulation cells are given in Table I.

The reconstruction itself requires the PS orbital, the atomic AE and PS partial waves, and the projector functions as input. The PS orbital is stored in Fourier space, so to evaluate the first term on the right-hand side of Eq. (1), we transform the PS orbital to real space, onto the logarithmic grid of the atomic code. Evaluation of the second term requires the atomic AE and PS partial waves and taking the scalar product of the projector functions and the PS orbital. The atomic functions are calculated on the logarithmic grid by the atomic code; the scalar product is evaluated in Fourier space. Each projector function is a radial function times a spherical harmonic.

TABLE I. Wavefunction cutoffs, density cutoffs, and cell sizes for the three test calculations (neon atom, gold atom, and TiO_2).

Test system	Wave function cutoff (Ry)	Density cutoff (Ry)	Cell size (a.u.)
Ne	30	200	30
Au	30	200	30
TiO_2	30	300	30

The AE-GTO calculations were performed using the GAUSSIAN 98 program package.[16] The molecular geometry for TiO_2 is taken from Ref. 21 (bond length: 3.06 a.u., bond angle: 110.0°). We use 6-311++G($3df$,$3pd$),[22] with a total of 159 basis functions, that include diffuse and polarization functions. The role of diffuse and polarization functions is to shift the electronic charge away from the nucleus, thus allowing higher flexibility in the representation of the total electron density. When using plane waves, this effect is automatically included in the computation due to the delocalized nature of the plane-wave basis. Therefore, we expect our AE-GTO orbitals to match the reconstructed ones in the limit of large basis sets.

IV. RESULTS

In this section we present comparison of FCAE orbitals obtained by the orbital reconstruction scheme based on the Blöchl transformation [Eq. (1)] and based on AE calculations. All the orbitals presented are normalized.

In Figs. 1, 2, and 3 we show comparisons of the radial projection of the $2s$,$2p$ orbitals of a neon atom, and the $5d$ orbital of a gold atom, respectively. The solid(dashed) line

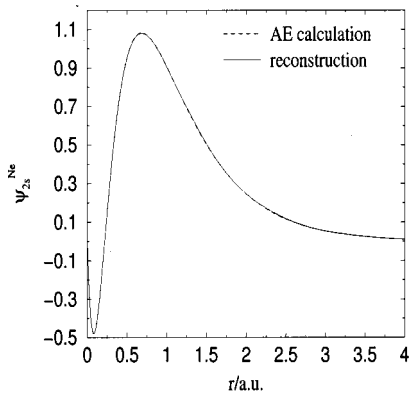

FIG. 1. Comparison of the all-electron orbital obtained by reconstructing the ultrasoft pseudo-wave function and by performing an all-electron calculation for the $2s$ orbital of a neon atom. The solid(dashed) line indicates the radial projection of the normalized reconstructed (all-electron) orbital. The two results compare extremely well, the two lines are hardly distinguishable.

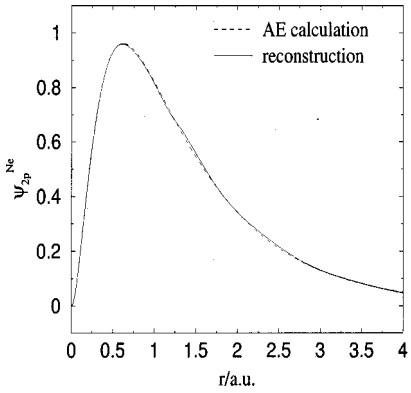

FIG. 2. Same as Fig. 1 for the $2p$ orbital of a neon atom. While the two curves are in excellent agreement, there are small oscillations of the reconstructed curve around the all-electron result. For an explanation, see the text.

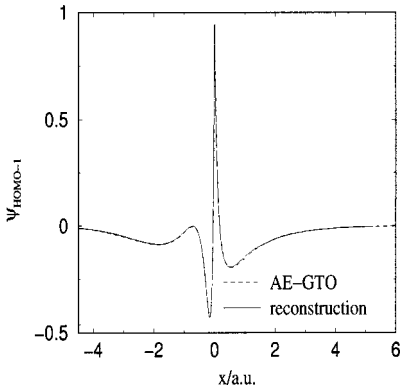

FIG. 4. Comparison of AE-GTO and reconstructed orbital corresponding to the HOMO-1. The normalized wave functions are plotted along the C_{2v} axis of the molecule, the titanium atom is at the origin, the projection of the Ti-O bonds point in the positive direction on the axis of the figure.

indicates the result of the reconstruction procedure (AE calculation). The reconstructed FCAE orbitals are in excellent agreement with the orbitals obtained from AE calculations. The lines are essentially indistinguishable. The integrated square differences between the two curves are on the order of 10^{-4} or less in all three cases, increasing in the order neon $2s$, neon $2p$, gold $5d$. In the case of the $2p$ orbital of the neon atom and the $5d$ orbital of the gold atom (shown in Figs. 2 and 3, respectively), the reconstructed AE result exhibits small oscillations around the result obtained from the AE calculation. These oscillations are also present in the PS orbitals. We attribute this effect to the finite size of the periodic cell, and not to the reconstruction procedure itself. In fact, for the $2p$ orbital of the neon atom we found these oscillations to decrease when using a larger cell.

In Figs. 4 and 5 we show two of the valence molecular orbitals of TiO_2 projected along the C_{2v} axis of symmetry. Of the 12 valence states of TiO_2 the first four are mainly s and p semicore states. Of the remaining states many have nodal planes that include the C_{2v} axis. We chose two states for which there is a significant contribution along the C_{2v} axis, namely, the second highest (HOMO-1) and the sixth highest (HOMO-5) occupied molecular orbitals. In both cases the agreement between the reconstructed FCAE orbital and the orbital obtained from the AE calculation is very good (note the difference between the scales of the two figures).

At a deeper analysis, small but visible differences appear between the reconstructed orbital and the AE-GTO result. In order to assess the nature of the differences between AE-GTO and the reconstruction we have calculated the root-mean-square deviation (RMSD) averaged over grid points within a sphere of radius R between the reconstructed orbital and the orbital calculated by AE-GTO. The results for the two states are shown in the upper panel of Fig. 6. The RMSD is larger in the nuclear core region, and it decreases as the radius of the sphere is increased.

In order to better understand the origin of this discrepancy, we have performed additional calculations on the Ti atom. In particular, we have calculated atomic orbitals using reconstruction, AE-GTO, and radial integration orbital on the same cubic grid as in the case of the molecule within a sphere of radius R. The RMSD as a function of R for the $3s$ orbital is shown in the lower panel of Fig. 6. The RMSD between the orbital resulting from radial integration and the reconstructed orbital is one order of magnitude smaller than either than between the reconstructed orbital and the AE-GTO orbital or between the radial integration and the AE-GTO orbital. The deviations decrease with radius, as in the case of the TiO_2 molecule. We conclude that the discrepancy between the orbital obtained by AE-GTO and the reconstructed orbital is due to inaccuracy of the GTO basis set in the core region.

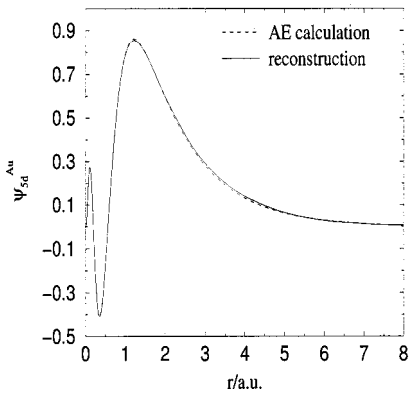

FIG. 3. Same as Fig. 1 for the $5d$ orbital of a gold atom.

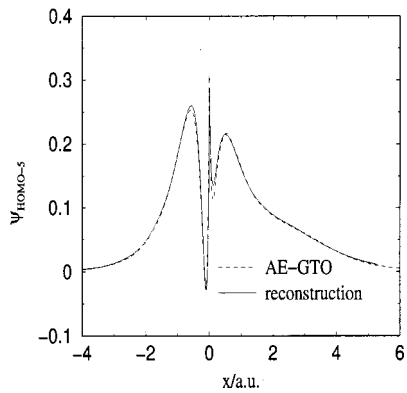

FIG. 5. Same as Fig. 4 for the HOMO-5 of TiO_2.

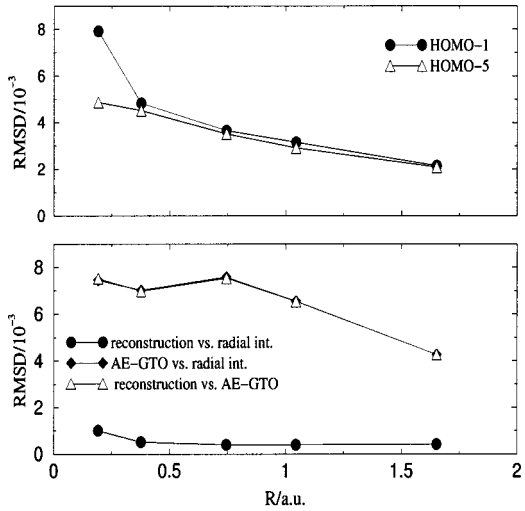

FIG. 6. The upper panel shows the root-mean-square deviation (RMSD) between the reconstructed orbitals and the corresponding orbitals resulting from the AE-GTO calculation for the HOMO-1 and HOMO-5 orbitals of TiO_2. The lower panel shows the RMSD between the reconstruction, radial integration, and AE-GTO calculation for the $3s$ orbital of the titanium atom. All deviations were calculated within a sphere of radius R.

V. CONCLUSION

In this paper we have tested whether the reconstruction of a frozen-core all-electron orbital from an ultrasoft pseudo-orbital is a numerically feasible operation.

The reconstruction scheme used here was based on a transformation written by Blöchl.[13] Blöchl uses this transformation to derive a frozen-core all-electron electronic structure method known as the projector-augmented wave. We have shown that the transformation that connects the pseudo-orbitals and the all-electron orbitals in the Blöchl formalism can be used to reconstruct all-electron orbitals from corresponding ultrasoft pseudo-orbitals.

We have compared reconstructed frozen-core all-electron orbitals to corresponding orbitals obtained from independent all-electron calculations for simple model systems; the $2s$ and $2p$ orbitals of a neon atom, the $5d$ orbital of a gold atom, and two valence states of the titanium dioxide molecule. Such a comparison shows that the reconstruction procedure used here is indeed a reliable method of obtaining all-electron orbitals from pseudo-orbitals.

We also note that our procedure is not restricted to plane-wave basis sets. In fact, running a pseudopotential calculation with a GTO basis set and reconstructing the corresponding all-electron orbital will result in an orbital with the right behavior at the nuclear positions, since in the reconstruction procedure the nuclear cusp is represented on a radial grid, not by GTOs. Such a procedure would lead to savings in basis set size. Furthermore, it is possible to construct potentials to represent atomic cores according to the projector-augmented wave or ultrasoft pseudopotential prescription in such a way that the frozen-core approximation is relaxed.

In a future publication[9] we will apply the methodology discussed in this work to calculate x-ray absorption spectra of condensed systems.

ACKNOWLEDGMENT

The authors would like to thank Dr. N. Marzari for helpful discussions.

[1] P. Hohenberg and W. Kohn, Phys. Rev. **136**, B664 (1964).
[2] W. Kohn and L. J. Sham, Phys. Rev. **140**, B1133 (1965).
[3] W. E. Pickett, Comput. Phys. Rep. **9**, 115 (1989).
[4] D. J. Singh, *Planewaves, Pseudopotentials and the LAPW Method* (Kluwer Academic, Dordrecht, 1994).
[5] U. von Barth and C. D. Gelatt, Phys. Rev. B **21**, 2222 (1980).
[6] N. A. W. Holzwarth, G. E. Matthews, R. B. Dunning, A. R. Tackett, and Y. Zeng, Phys. Rev. B **55**, 2005 (1997).
[7] T. Gregor, F. Mauri, and R. Car, J. Chem. Phys. **111**, 1815 (1999).
[8] J. Stöhr, *NEXAFS Spectroscopy* (Springer, Berlin, 1992).
[9] B. Hetényi, F. De Angelis, P. Giannozzi, and R. Car (unpublished).
[10] C. J. Pickard and F. Mauri, Phys. Rev. B **63**, 245101 (2001).
[11] C. G. Van de Walle and P. E. Blöchl, Phys. Rev. B **47**, 4244 (1993).
[12] A. Stirling, A. Pasquarello, J.-C. Charlier, and R. Car, Phys. Rev. Lett. **85**, 2773 (2000).
[13] P. E. Blöchl, Phys. Rev. B **50**, 17953 (1994).
[14] D. Vanderbilt, Phys. Rev. B **41**, 7892 (1990).
[15] D. R. Hamann, M. Schlüter, and C. Chiang, Phys. Rev. Lett. **43**, 1494 (1979).
[16] M. J. Frisch, G. W. Trucks, H. B. Schlegel *et al.*, GAUSSIAN 98, Gaussian, Inc., Pittsburgh, PA, 1998.
[17] K. Laasonen, A. Pasquarello, R. Car, C. Lee, and D. Vanderbilt, Phys. Rev. B **47**, 10142 (1993).
[18] L. Kleinman and D. M. Bylander, Phys. Rev. Lett. **48**, 1425 (1982).
[19] P. E. Blöchl, Phys. Rev. B **41**, 5414 (1990).
[20] J. P. Perdew, J. A. Chevary, S. H. Vosko, K. A. Jackson, M. R. Pederson, D. J. Singh, and C. Fiolhais, Phys. Rev. B **46**, 6671 (1992).
[21] M. V. Ramana and D. H. Phillips, J. Chem. Phys. **88**, 2637 (1987).
[22] M. J. Frisch, J. A. Pople, and J. S. Binkley, J. Chem. Phys. **80**, 3265 (1984).